JOURNAL OF GEOPHYSICAL RESEARCH, VOL. 113, C04022, doi:10.1029/2007JC004322, 2008

Laboratory experiments on mesoscale vortices colliding with an island chain

Aya Tanabe[1] and Claudia Cenedese[2]

Received 5 May 2007; revised 12 September 2007; accepted 13 December 2007; published 17 April 2008.

[1] The present laboratory study investigates the behavior of a self-propagating barotropic cyclonic vortex colliding perpendicularly with aligned circular cylinders and determines the condition for a vortex to bifurcate and split into multiple vortices and/or to generate dipoles downstream of the cylinders. During the experiments, four parameters were varied: G, the gap width between the cylinders; d, the diameter of the incident vortex; Y_{dis}, a parameter expressing the initial vortex positions; and D_{isl}, the total length of the "middle" island. It has been observed that as long as $0.1 < G/d \leq 0.4$, the vortex fluid was funneled between two cylinders at one of the gaps and a dipole generally formed, much like water ejected from a circular nozzle generates a dipole ring. After the dipole formed, the cyclonic part of the dipole became dominant and self propagated away from the cylinders. Furthermore, in some experiments having $0.2 < D_{isl}/d \leq 0.5$, after a weak dipole formed, the remnant of the original vortex moved zonally "south." When the remnant of the vortex came in contact with a new cylinder, fluid peeled off the outer edge of the vortex and a so-called "streamer" went around the cylinder in a counterclockwise direction. Under the right conditions, this fluid formed a new cyclonic vortex in the wake of the cylinder, causing bifurcation of the original vortex into two vortices, as observed in previous studies. In general, independently of the configurations and Y_{dis}, the number of cyclonic vortices downstream of the cylinders was one, either originating from the dipole or generated by the bifurcation of the original vortex. The vortex center position, radius, and circulation, before and after the interaction, were computed from its velocity field. It was found that for $0.1 < G/d \leq 0.4$, intense vortices experienced greater amplitude loss than weak vortices. The formation of both a dominant cyclone and an anticyclone (i.e., a dipole) downstream of the aligned cylinders, representing an island chain, is in agreement with recent oceanic observations of North Brazil Current (NBC) rings interacting with the Lesser Antilles in the Eastern Caribbean Sea. Since the passages of the Lesser Antilles have values of $0.07 \leq G/d \leq 0.3$, the oceanic observations might be explained by the experimental results reported in this paper.

Citation: Tanabe, A., and C. Cenedese (2008), Laboratory experiments on mesoscale vortices colliding with an island chain, *J. Geophys. Res.*, *113*, C04022, doi:10.1029/2007JC004322.

1. Introduction

1.1. Oceanographic Context

[2] Mesoscale vortices have recently been recognized to play an important role in the redistribution and transport of water properties (e.g., temperature, salinity) around the oceans. The interaction of vortices with seamounts, submerged ridges, or islands might result in an enhanced and localized transfer of anomalous fluid from the vortices to the surrounding environment. In addition, the interaction could result in the formation of new vortices downstream topographic obstacles and/or the complete destruction of the incident vortices. This topic has been investigated for the past several decades, looking for example at Meddies in the eastern North Atlantic, Agulhas rings in the eastern South Atlantic, and North Brazil Current (NBC) rings in the western tropical Atlantic. In particular, in the current study, we will focus on the behavior of the last kind of vortices, NBC rings, which interact with the Lesser Antilles island chain.

[3] It is believed that NBC rings are one of the leading mechanisms for transporting the upper ocean equatorial and South Atlantic water into the North Atlantic as part of the Meridional Overturning Cell (MOC). The MOC transports cold deep water southward across the equator and, to be balanced, transports upper ocean South Atlantic waters northward. In the upper layers, the NBC is a northward flowing western boundary current that carries warm water across the equator along the coast of Brazil (Figure 1). Near 5°–10°N, the NBC separates sharply from the coastline and

[1]Department of Mathematics, Imperial College London, London, UK.
[2]Department of Physical Oceanography, Woods Hole Oceanographic Institution, Woods Hole, Massachusetts, USA.

0148-0227/08/2007JC004322$09.00

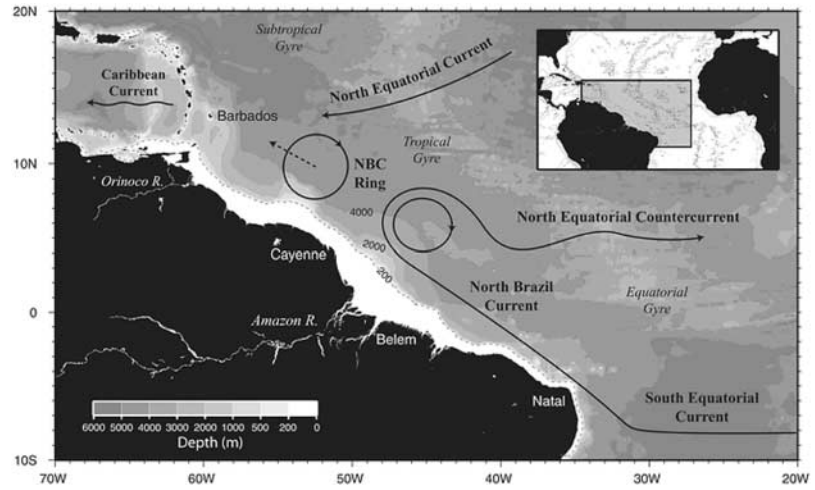

Figure 1. Sketch of the upper-ocean circulation in the western tropical Atlantic from *Fratantoni and Glickson* [2002].

retroflex to feed the eastward North Equatorial Counter Current (NECC) [*Jones et al.*, 1990]. During its retroflection, the NBC occasionally pinches off isolated anticyclonic warm-core vortices. The majority of those have a surface expression, exceed 450 km in overall diameter and 2 km in vertical extent, and swirl at speed approaching 100 cm s^{-1}. These NBC rings move north-westward toward the Caribbean at 8–17 cm s^{-1} on a path parallel to the coastline. As part of the MOC, in most cases they then interact with a complex island chain, the Antilles islands [*Fratantoni and Richardson*, 2006], and enter the Caribbean Sea. (Episodically, they enter the North Atlantic subtropical gyre). The inflow into the Caribbean Sea ultimately feeds the Florida Current which is now recognized to be a fundamental passage for northward transport of upper ocean waters in the global thermohaline circulation. Therefore, the Atlantic MOC (hence NBC rings) is an important element of the global thermohaline circulation and a fundamental component of the global climate system.

[4] Recent observations (see Figure 2) reveal that relatively large (average diameter 200 km) energetic anticyclonic vortices were found downstream of the Antilles islands in the Eastern Caribbean Sea, and they translated westward whereas cyclonic vortices were observed primarily near boundaries in the Eastern Caribbean Sea [*Richardson*, 2005]. To date, it is still not clear whether or not such large anticyclonic and cyclonic vortices observed in the Eastern Caribbean Sea have been produced as a consequence of the interaction between NBC rings and the Antilles islands, and if so, what the formation mechanism is. In the present work, we shall try to answer part of this question through laboratory experiments.

1.2. Dynamical Background

[5] Recently, several studies have focused on the interaction of vortices with islands or seamounts and the possible "bifurcation" of the original vortex into multiple vortices. In the laboratory, the interaction of a cyclonic vortex with vertical cylinder(s) has been investigated by *Cenedese* [2002], *Adduce and Cenedese* [2004], and *Cenedese et al.* [2005]. Numerical modeling studies investigating vortex-island(s) interaction have been carried out by *Simmons and Nof* [2000, 2002], *Dewar* [2002], *Herbette et al.* [2003], *Wang and Dewar* [2003], and E. Chassignet (personal communication, 2004). Finally, the motion of a vortex near two cylinders, both for a line vortex and a patch of constant vorticity, has been investigated analytically by *Johnson and McDonald* [2004a, 2004b, 2005]. (A line vortex is an idealized, mathematical vortex consisting of the limit of the contraction of a vortex tube to a curve in space. The flow surrounding the curve is assumed irrotational [*Batchelor*, 1967].) Below, we will summarize only those studies of relevance to the present experiments.

[6] *Cenedese* [2002] suggested an analytical approach that describes the interaction of a monopolar vortex with a vertical cylinder. They started by calculating the circulation around a cylinder for a single layer of homogeneous fluid and derived a fundamental dynamic constraint by integrating the tangential component of the momentum equation around the cylinder [*Godfrey*, 1989; *Pedlosky et al.*, 1997]. The equation for the circulation around the cylinder in the case of no-slip boundary condition, i.e., the velocity $\mathbf{u}$ is identically equal to zero on the boundary and consequently on the closed circuit C, is given by:

$$\oint_C Diss(\mathbf{u}) \cdot \hat{t} ds = \oint_C \nu \nabla^2 \mathbf{u} \cdot \hat{t} ds = \oint_C \nu \frac{\mathrm{v}}{\delta^2} R \, d\theta = 0, \quad (1)$$

where only lateral friction has been considered, $Diss(\mathbf{u}) = \nu\nabla^2\mathbf{u}$; the horizontal thickness of the streamer is scaled with the boundary layer thickness δ; the tangential component of the velocity $\mathbf{u}$ within the boundary layer thickness is scaled with a characteristic velocity v; and considering the cylinder arc element $ds = Rd\theta$, where R is the cylinder radius. When a vortex interacts with a cylinder (1) must hold. As observed by *Cenedese* [2002], the flow within the outer edge of the cyclone encounters the cylinder, and stagnates somewhere on C. Therefore, it separates from the vortex to form what they define as a "streamer" and moves around the cylinder with a counterclockwise velocity v_s through an angle θ_s. The remaining fluid continues as part of the original vortex

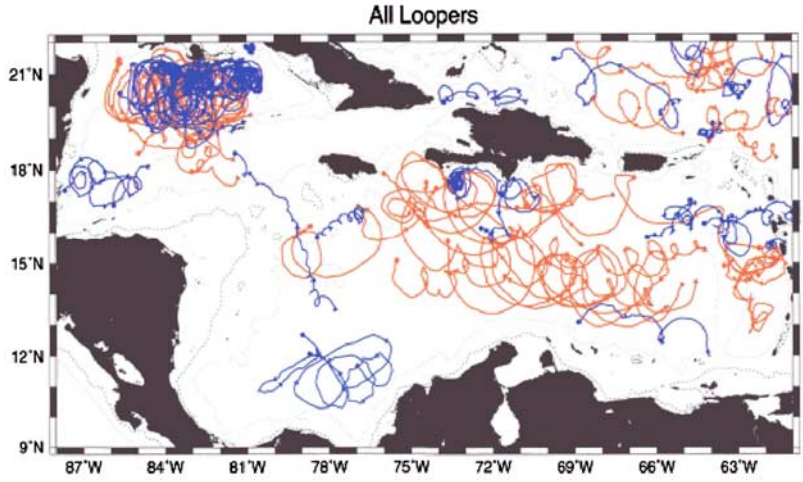

Figure 2. Drift trajectories of 28 cyclones (blue) and 29 anticyclones (red). Anticyclones seem to be dominant in the Eastern Caribbean Sea between 65°W and 75°W from *Richardson* [2005].

with a cyclonic azimuthal velocity v_e and interacts with the cylinder over an angle θ_e. Finally, considering that R, δ, and ν are constants, (1) gives

$$\oint_C v\, d\theta = 0, \tag{2}$$

and, integrating (2) around the circuit C we obtained

$$v_e\, \theta_e = v_s\, \theta_s. \tag{3}$$

Equation (3) implies that the dissipation of fluid within the vortex interacting with an arc of the cylinder given by $R\theta_e$ has to be balanced by the dissipation of fluid within the streamer going around the cylinder in the opposite direction (counterclockwise) over an arc $R\theta_s$. Equation (3) was also used in the work of *Cenedese* [2002] to calculate the value of the Reynold number defined as

$$Re = \frac{v_s L_{\max}}{\nu}, \tag{4}$$

where v_s is the velocity of the streamer going around the cylinder, ν is the kinematic viscosity and $L_{\max} = \max [D, d]$ is the larger lengthscale between the cylinder, D, and the vortex, d, diameter. In equation (3), v_e can be expressed as $v_e = \Omega_e r$, where Ω_e is the angular velocity of the vortex and r is the vortex radius. By single substitution, (4) becomes

$$Re = \Omega_e \frac{\theta_e}{\theta_s} \frac{r L_{\max}}{\nu} = \Omega_e \frac{\theta_e}{\theta_s} \frac{r}{R} \frac{R L_{\max}}{\nu}, \tag{5}$$

where the Reynolds number is now a function of the ratio of the vortex to the cylinder radius. *Cenedese* [2002] observed that when the streamer velocity v_s was large enough, $400 \leq Re \leq 1100$, a new cyclonic vortex formed in the wake of the cylinder. Using equation (5), this regime corresponded to values of $0.2 \leq R/r \leq 1.0$, for a self-propagating vortex. These results, indicating that bifurcation occurs approximately for $400 \leq Re \leq 1100$, are in agreement with previous studies of uniform flow past a cylinder in a rotating environment, and therefore they suggest that the new vortex in the wake of the cylinder was formed in a similar fashion as those in the Karman vortex street.

[7] Furthermore, the interaction of a monopolar, self-propagating barotropic cyclonic vortex with two circular cylinders was investigated in the laboratory by *Cenedese et al.* [2005]. In a similar way as described above for the case of a single cylinder, after the vortex came in contact with the two cylinders, provided the "streamer" (or two "streamers") velocity v_s was large enough (i.e., $400 \leq Re \leq 1100$), the "streamer(s)" formed a new cyclonic vortex (or two new vortices) in the wake of the cylinder(s). One of the remarkable observations of *Cenedese et al.* [2005] is that in few experiments, the flow within the vortex was funneled in the form of a jet between the two cylinders and formed a dipole vortex, much like water ejected from a circular nozzle generates a dipole ring. This behavior occurred provided that $0.25 \leq G/d \leq 0.4$, and $Re_G > 200$, where G is the separation between the two cylinders, d is the diameter of the incident vortex, $Re_G = U_G G/\nu$ is the Reynolds number based on a length scale $\sim O(G)$, and U_G is the maximum velocity of the vortex fluid in the gap. The size of the new cyclonic and anticyclonic vortices (i.e., a dipole) downstream of the two cylinders was smaller than that of the original vortex. Dimensional analysis [*Afanasyev and Korabel*, 2004] shows that jet-like flows are governed by the value of the Reynolds number. In the experiments of *Cenedese et al.* [2005], the jet in the gap generated vorticity as it entered the quiescent fluid downstream of the cylinders, provided that the Reynolds number was large enough. (The sheared velocity profile of the jet, due either to the gap walls or the quiescent fluid, presents opposite sign vorticity on each side of the central maximum velocity.) This vorticity was in the form of two vortices of opposite signs constituting a vortex dipole. A review of vortices and dipoles is given by *Voropayev and Afanasyev* [1994] and more recent studies on dipole formation were carried out by *Afanasyev and Korabel* [2004] and *Afanasyev* [2006].

[8] A numerical investigation of the interaction of both a self-propagating and an advected vortex with multiple

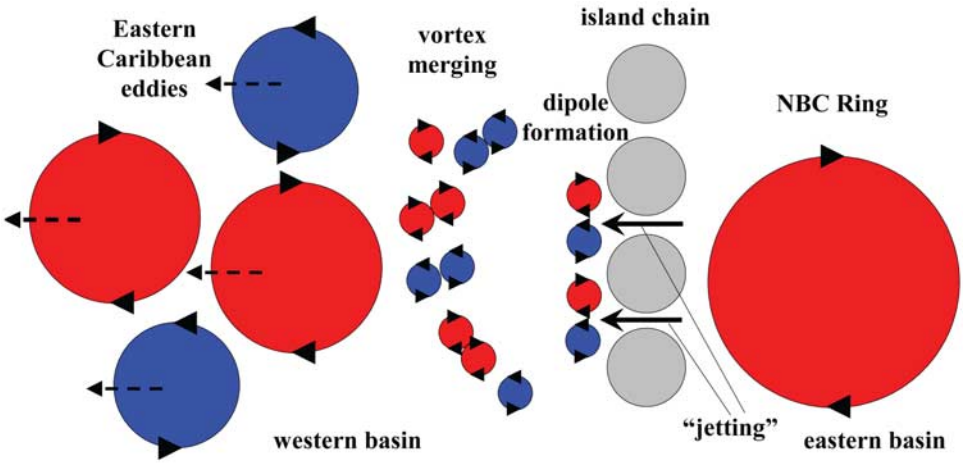

Figure 3. Sketch illustrating a possible formation mechanism for the large anticyclonic and cyclonic vortices observed in Eastern Caribbean Sea.

islands was done by *Simmons and Nof* [2002]. The islands were represented by thin vertical walls aligned in the north-south direction with gaps having a width of 20% of the vortex diameter. Their results indicated that if the individual islands were small compared with the vortex radius (e.g., $L/R_i = 0.3$, where L is the island length and R_i is the initial vortex radius), the vortex reorganized in the basin downstream of the islands as a single structure, whereas it always split into multiple vortices if the islands were large (e.g., $L/R_i = 1.5$). (It is worth noticing that the definition of R_i is not strictly defined in the work of *Simmons and Nof* [2002], hence R_i and $d/2$, defined by *Cenedese et al.* [2005] are not necessarily equal.) Moreover, intense vortices experienced relatively greater amplitude loss than weak vortices.

[9] Finally, numerical simulation of the North Atlantic using the Miami Isopycnic Coordinate Ocean Model (MICOM) (E. Chassignet, personal communication, 2004) show that after the interaction of a NBC ring with the Antilles islands, the original vortex seems to "bifurcate" and generate a new vortex in the wake of the islands. Vortices of opposite sign (i.e., cyclonic) than the original vortex are observed downstream of the island passages. To the authors' knowledge, a detailed analysis of this bifurcation mechanism and possible dipole formation has not been carried out through an investigation of the MICOM output.

1.3. Present Study: Working Hypothesis

[10] On the basis of the previous studies described above, we formulated the following hypothesis: Since the Lesser Antilles have passages' between 30 and 60 km wide and the approaching NBC vortices' diameter varies between 200 and 400 km [see *Fratantoni and Richardson*, 2006], G/d lies in the range of 0.07–0.3. Although this range is not exactly the same as $0.25 \leq G/d \leq 0.4$ obtained by *Cenedese et al.* [2005], it is natural to anticipate that dipole formation is likely to occur downstream of the Lesser Antilles' passages. Assuming that several pairs of dipoles are formed at the western side of the islands by several vortex-islands interactions, we expect that transition from small-scale vortices to large-scale structures will occur by the merging of vortices of like sign (Figure 3), as suggested by the laboratory experiments of *Linden et al.* [1995]. When rotation is present, the scale to which the vortices grow is determined by instability processes that inhibit vortices to grow to scales larger than the Rossby radius of deformation [*Linden et al.*, 1995]. The coalescence of same sign vortices is similar to the well-known feature of inverse energy cascade in two-dimensional flow [*McWilliams*, 1984]. Finally, vortices having a diameter of the order of the Rossby radius of deformation will form and drift westward due to the planetary β-plane (Figure 3).

[11] The focus of the present work is to extend the study of *Cenedese et al.* [2005] to test the above working hypothesis and, in particular, to extensively investigate the formation of dipoles downstream of multiple islands. *Cenedese et al.* [2005] seldom observed the formation of a single dipole (only in four out of 48 experiments) and never observed multiple dipoles. The formation of a dipole was an "unexpected and revealing result," as described by *Cenedese et al.* [2005], and the possible parameter ranges for a dipole to occur were not fully investigated. Hence, the motivation for the present work, which focuses specifically on the dipole formation and, in particular, seeks the formation of multiple dipoles from a single vortex, and the possible interaction of these dipoles, as described in the working hypothesis and in Figure 3. The present work differs substantially from *Cenedese et al.* [2005] in that it aims to examine whether a single barotropic cyclonic vortex can bifurcate into several dipoles. This behavior could not be observed by *Cenedese et al.* [2005] because their configuration had only a single gap, while the present configuration, with multiple gaps, can allow for the formation of multiple dipoles. In particular, we expect that, for small values of D_{isl}/d, the original vortex may form several dipoles in contiguous gaps. Another significant difference between the present study and *Cenedese et al.* [2005] is that here we investigate the fate of a vortex interacting with an "island chain" for values of $G/d \rightarrow 0$. We expect the bifurcation and dipole formation mechanisms to stop occurring as $G/d \rightarrow 0$. Again, this behavior could not be investigated by *Cenedese et al.* [2005] because in their work, for values of $G/d \rightarrow 0$, the

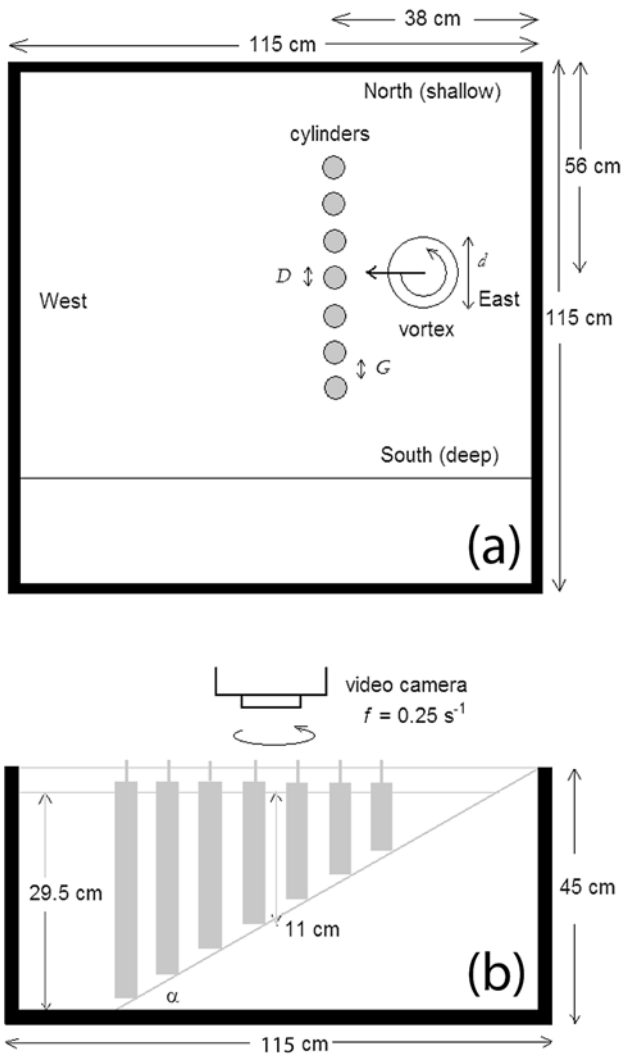

Figure 4. Sketch of the experimental apparatus: (a) top view; (b) side view.

two islands behaved like a single island and the original vortex could still bifurcate into two vortices (see their section 3.3).

[12] The rest of this paper is organized as follows. In section 2, the apparatus used for the experiments and the measurements taken are described. In section 3, we report the phenomena and the evolution of a typical flow seen in the experiments. We compare the results with previous laboratory and numerical studies in section 4 and with observations in section 5. Finally, this paper concludes in section 6 with a summary and further discussion of the experimental results presented in section 3.

2. Experiments

2.1. Experimental Apparatus

[13] The experiments were performed in a square tank of depth 45 cm, with length and width of 115 cm. "Top-view" and "side-view" illustrations of the apparatus are shown in Figures 4a and 4b, respectively. The apparatus was mounted concentrically on a 2-m-diameter rotating turntable with a vertical axis of rotation. The sense of rotation of the turntable was counterclockwise. A square tank was used to avoid optical distortion from side views associated with a circular tank. The tank had a sloping bottom which makes an angle α to the bottom of the tank in order for a vortex to self-propagate leftward when looking upslope [*Cushman-Roisin*, 1994]. Although the exact equivalence between the β-plane effect and the sloping topography effect depends on the smallness of the angle of the slope α and the Rossby number *Ro*, we will name for reference north the shallowest part of the tank. Hence, east is to the right when looking upslope, west is to the left, and south is the deepest part of the tank. The tank was filled with fresh water, which was initially in solid body rotation. Seven circular cylinders whose diameter is D were aligned in the north-south direction, and each of them was separated by a gap G as shown in Figure 4a. The position of the central cylinder, the fourth one from north (or south), was always fixed. However, the position of the other cylinders was changed to vary the value G. The depth of the water at the central cylinder, h_0, was 11 cm which was much larger than the Ekman layer depth $\delta_{Ek} = \sqrt{2\nu/f} \approx 3$ mm, where ν is the kinematic viscosity of the water and f is the Coriolis parameter. The bottom of each cylinder was sliced at an angle to remain in contact with the sloping bottom.

[14] A barotropic cyclonic vortex was generated by placing an ice cube in the water [*Whitehead et al.*, 1990], a method dynamically similar to withdrawing fluid from a sink positioned on the sloping bottom. The water surrounding the ice cube, due to conduction, becomes colder than the surrounding water and sinks as a cold plume, forming a cold dense lens within the thin bottom Ekman layer. The cold dense plume entrains ambient water inducing inward velocities along the entire column depth above the bottom lens that, influenced by the Coriolis force, generates a cyclonic vortex. In order to conserve mass, the dense fluid in the bottom Ekman layer flows radially outwards with a rapid velocity in comparison to the rotation period of the tank and thus a dense anticyclonic vortex does not form on the bottom. The fluid flowing radially outward from the bottom lens moves slowly downslope within the Ekman layer and then veers right influenced by the Coriolis force, as shown

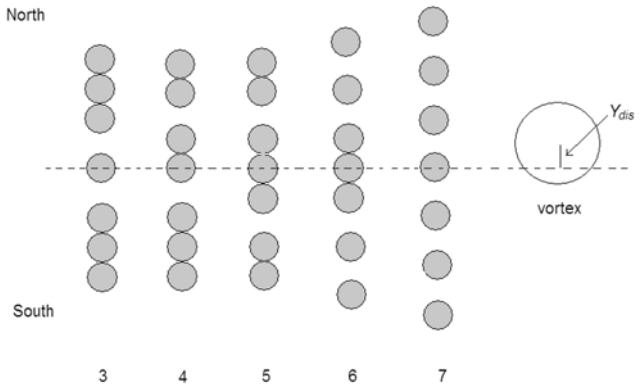

Figure 5. Five configurations of the cylinders used in the experiments. The position of the fourth cylinder from north (or south) was kept fixed.

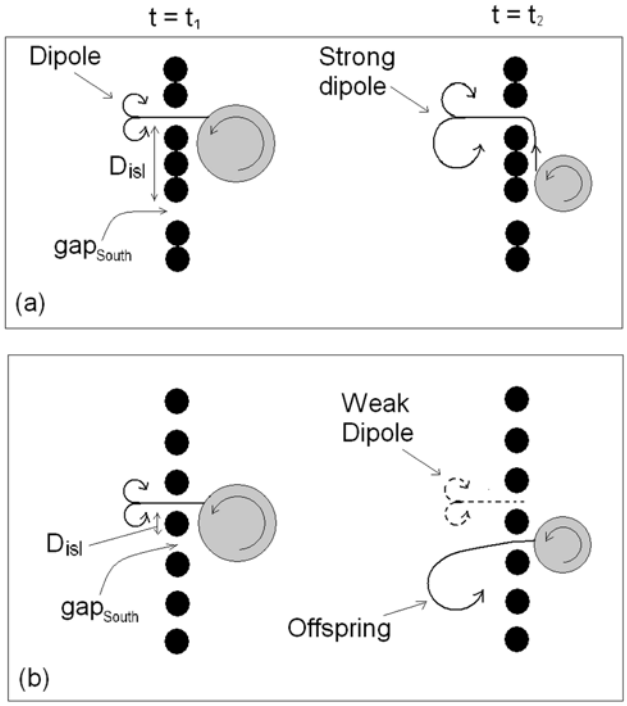

Figure 6. Sketch of the offspring (i.e., new vortex) formation for $0.1 < G/d \leq 0.4$ and (a) for all experiments with $0.5 < D_{isl}/d \leq 1.5$ and for some experiments with $0.2 < D_{isl}/d \leq 0.5$ (configuration 5 in this illustration); (b) sketch of offspring formation from the remnant of the original vortex at $\text{gap}_{\text{south}}$ for some experiment with $0.2 < D_{isl}/d \leq 0.5$ (configuration 7 in this illustration). Here t_1 and t_2 ($t_1 < t_2$) are two successive time frames.

in Figure 8. The fluid within the dense lens moves downslope together with the established barotropic cyclonic vortex above it. Influenced by the Coriolis force, both the cyclonic water column and the cold lens change their direction and start drifting westward with a very small meridional displacement. Although NBC rings are anticyclonic vortices, in the laboratory it was not possible to reproduce stable barotropic anticyclones as they tend to be centrifugally unstable [*Kloosterzil and van Heijst*, 1991] and become nonaxisymmetric in a few rotation periods. Furthermore, NBC rings have a baroclinic structure and move within a stratified fluid. As shown by *Cenedese* [2002], the use of cyclonic vortices does not limit the generality of the results, which can be easily extended to anticyclones. In particular, the circulation equation around the cylinder, equation (1), and the equation relating the streamer velocity to the vortex velocity, equation (3), still hold for anticyclones. However, in present study, we did not investigate the effect of a stratified environment and the influence of the advection mechanism on the interaction. Lack of stratification is possibly one of the weakest points of our model but the good agreement between the experimental results obtained by *Cenedese* [2002], *Adduce and Cenedese* [2004], *Cenedese et al.* [2005], and the oceanic observations suggests that stratification does not invalidate the relevance of the results discussed here.

[15] For all the experiments, the Coriolis parameter f was fixed at 0.25 s^{-1}, and $\nu = 0.01$ cm^2 s^{-1}. The bottom slope was set at $s = \tan\alpha = 0.5$ so that the self-propagating vortex moved westward with a speed $U \approx 0.2$ cm s^{-1}. The distance from the center of the incident vortex to the east-west axis passing through the center of the "middle" cylinder, Y_{dis}, was chosen to be small and was defined positive (negative) if the vortex center was northern (southern) of the east-west axis (Figure 5). The vortex was produced approximately 20 cm westward of the eastern wall of the tank, and moved 20 cm westward and interacted with the chain of cylinders before the spindown time $\tau = h_0/\sqrt{\nu f} \approx 200$ s. The diameter of the cylinders, D, is 3.3 cm. Three values for the size of the gaps, $G = 0.7$, 1.5, 3 cm and five types of configurations of the cylinders (Figure 5) were studied. The total length of the "middle" island, D_{isl}, changed in the different configurations used. In particular, $D_{isl} = D = 3.3$ cm for configuration 3 and 7, $D_{isl} = 2D = 6.6$ cm for configuration 4, and $D_{isl} = 3D = 9.9$ cm for configurations 5 and 6. The azimuthal velocity profile of the vortex in the experiments, v_θ, is similar to that of a Rankine vortex with an approximately constant vorticity (solid body rotation) for $0 \leq r' \leq r'_{\max}$ and a velocity which decays roughly like $1/r'$ for $r' > r'_{\max}$, where r' is the radial coordinate originating in the vortex center. We define the vortex radius r to be not $r'_{\max}$, where the azimuthal velocity of the vortex is maximum, but the radial distance (from the center of the vortex) where the velocity has decayed by approximately 30% (i.e., $r = r'_{\max}/0.7$). This definition for the vortex radius is same as the one in the work of *Adduce and Cenedese* [2004] and *Cenedese et al.* [2005]. The incident vortex diameter d ranged between 7.6 and 19 cm due to nonuniformity of the size of the ice cubes used.

2.2. Measurements

[16] A video camera was mounted above the tank and was fixed to the turntable so that we were able to observe the flow in the rotating frame. The vortex was made visible by using dye (food coloring) and/or by adding buoyant paper pellets on the free surface. The motion of the dyed vortex was also observed from the side of the tank. An image-processing software, DigiFlow, was used to perform particle tracking on the paper pellets and calculate the velocity field by mapping the individual velocity vectors onto a rectangular grid using a spatial average over 2 cm and a time average over 10 s. Once the gridded velocity was obtained, quantities such as the vortex position (center), the radial distance r' where the vortex velocity is maximum (i.e., $r'_{\max}$), and the circulation of the vortex, before and after the interaction with the cylinders, were computed. The circulation of a vortex is defined as

$$\Gamma = A \sum_i \omega_i, \tag{6}$$

where A is the area of the single grid square, and ω_i is the relative vorticity at each grid point with $r' \leq r$. By simply looking at the video tape, it is possible to quantify the number of new vortices (i.e., offsprings) generated by the interaction, N, whether or not a dipole (or several dipoles) formed, and whether or not there was a "backward" flow,

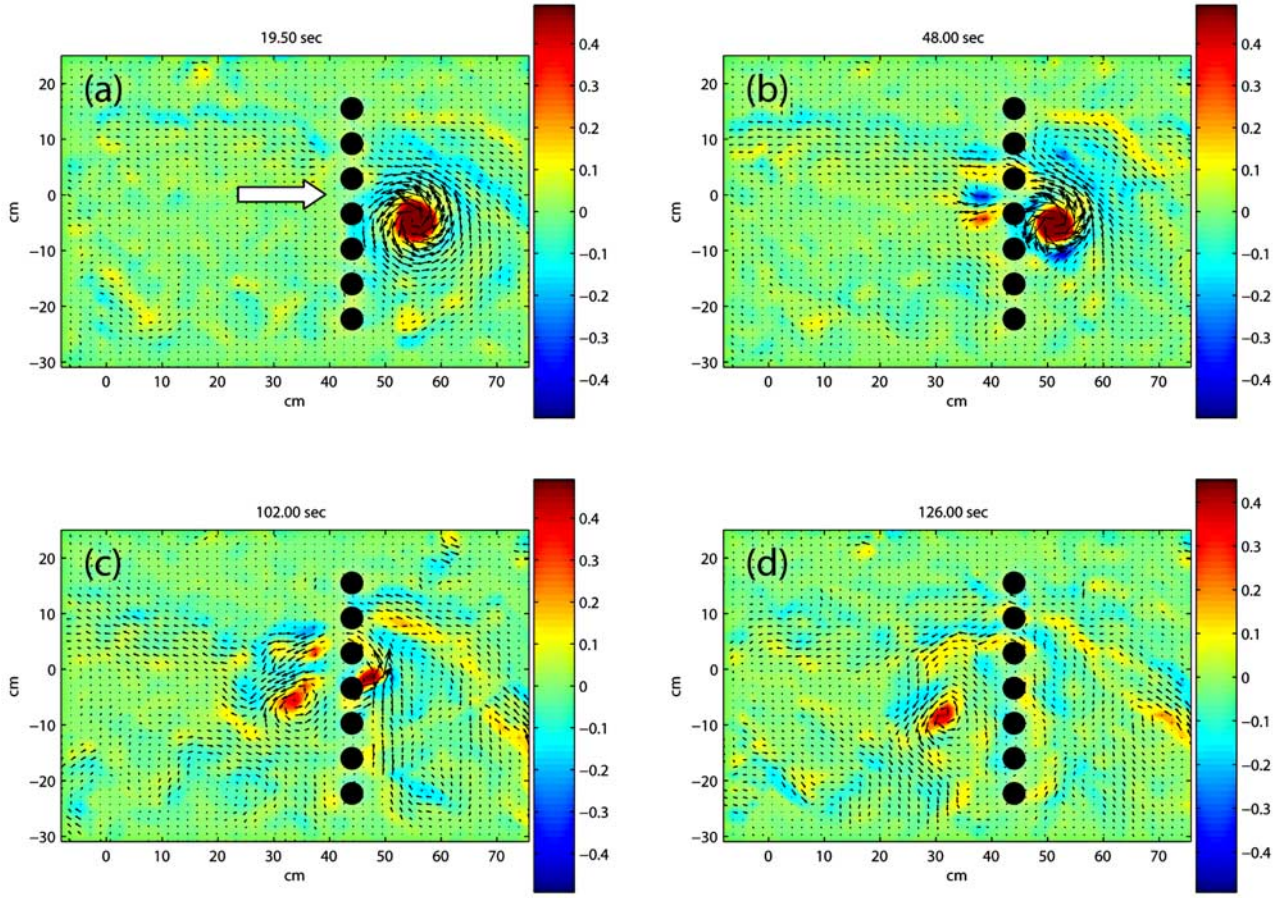

Figure 7. Velocity shown by the arrows (cm s^{-1}) and vorticity shown by the colors (s^{-1}) for a configuration 7 experiment with $G/d = 0.23$ and $D_{isl}/d = 0.26$: (a) just before the interaction ($t = 19.5$ s); (b) during dipole formation ($t = 48$ s); (c) when the cyclonic part became dominant ($t = 102$ s); (d) during the offspring (i.e. new vortex) formation ($t = 126$ s). The solid white arrow in Figure 7a indicates the gap where the dipole will form.

defined as fluid flowing between the cylinders from west to east.

3. Experimental Results

3.1. Dipole Formation and Vortex Bifurcation ($0.1 < G/d \leq 0.4$)

[17] For values of $0.1 < G/d \leq 0.4$ and for all experiments with $0.5 < D_{isl}/d \leq 1.5$ and for some experiments with $0.2 < D_{isl}/d \leq 0.5$, as soon as a vortex encountered the cylinders, vortex fluid was funneled, and a jet formed in the gap aligned with the northernmost part of the vortex were the azimuthal velocity was directed westward. As shown in Figure 6a, the fluid in the jet moved through the gap and almost always formed a strong dipole downstream of the cylinders, for all the configurations of the cylinders (Figure 5) and for all the initial vortex position attempted, i.e., Y_{dis}. Figures 7 and 8 show two laboratory experiments with $G/d = 0.23$ and 0.30, respectively. Figure 7 shows the velocity and vorticity fields for an experiment with configuration 7, while Figure 8 shows an experiment with configuration 3 in which a white sloping bottom and dye were used to visualize the flow. A dipole is clearly visible downstream of the third gap (from north) in Figure 7b (i.e., a pair of red and blue vortices) and downstream of the first gap (from north) in Figure 8b (i.e., a "mushroom"-shaped pair of vortices). The gap where the dipole formed (white arrow in Figures 7a and 8a) is aligned with the northernmost part of the vortex where the azimuthal velocity is directed into the gap (i.e., east-west). After a dipole formed, the anticyclonic part of the dipole was usually weaker than the cyclonic counterpart, and it slowly weakened in time. The cyclonic part of the dipole became dominant (Figures 7c and 8c), eventually the anticyclonic part of the dipole disappeared as well as the original vortex, and the interaction resulted in the production of a relatively large cyclonic vortex (Figures 7d and 8d). The formation of two or more dipoles never occurred in contiguous gaps although the vortex extended for several cylinder and gap lengths.

[18] For values of $0.1 < G/d \leq 0.4$ and $0.2 < D_{isl}/d \leq 0.5$ (configurations 3 and 7), the interaction was either similar to the one described above and resulted in a cyclonic vortex that was generated directly from the cyclonic part of the dipole, or in some experiments the dipole formation was interrupted generating a weak dipole. As shown in Figure 6b, the original vortex started forming the dipole as described above, but after a short period, it moved south due to its image vortex and the fluid from the vortex stopped supplying fluid

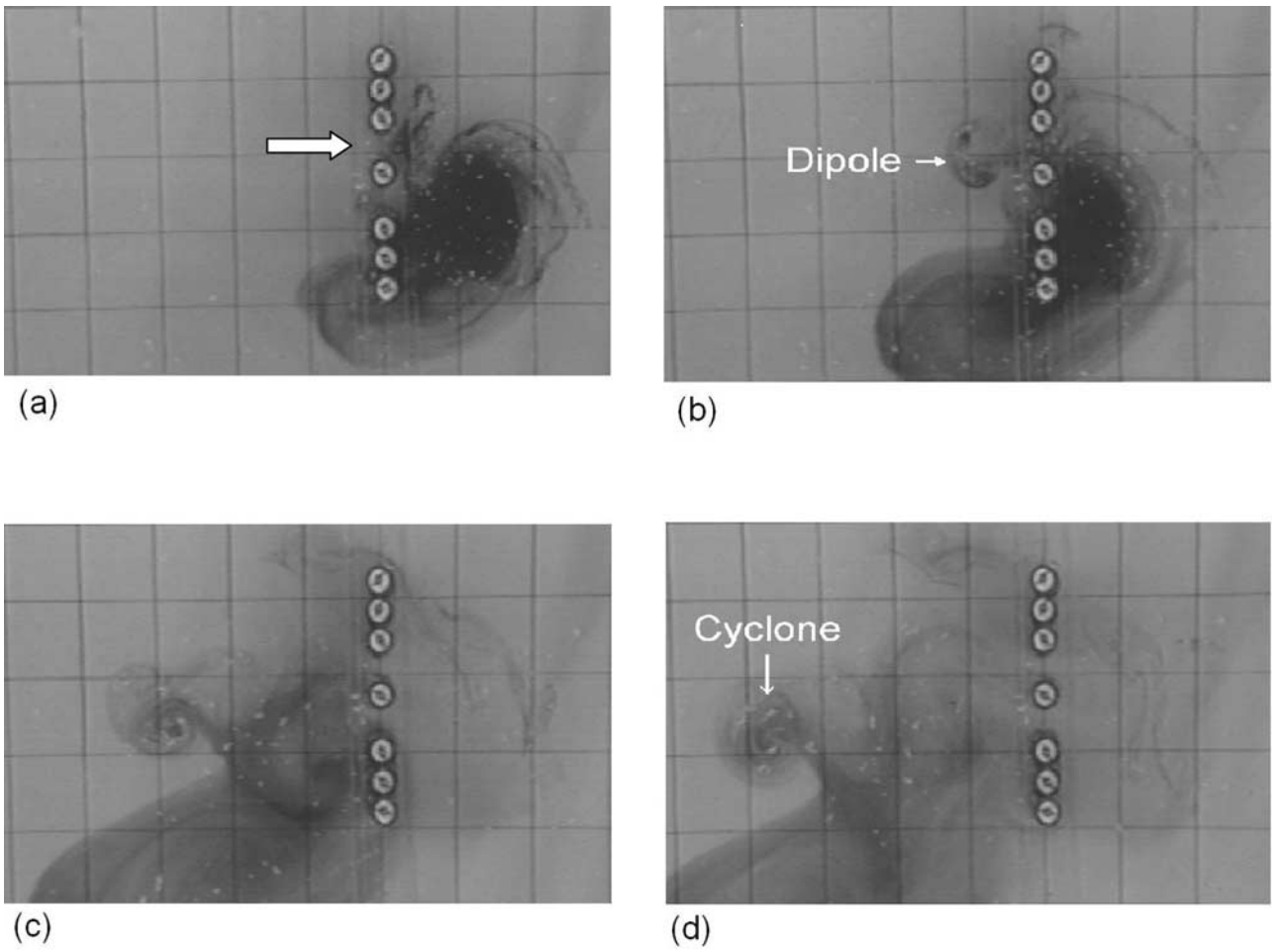

Figure 8. A dye experiment for a configuration 3 with $G/d = 0.30$ and $D_{isl}/d = 0.30$: (a) just before the interaction ($t = 7$ s); (b) dipole formation ($t = 48$ s); (c) the cyclonic part became dominant ($t = 144$ s); (d) offspring (i.e., new vortex) formation ($t = 182$ s). The dark fluid moving southwestward is the dense fluid within the Ekman layer as discussed in section 3.1. The solid white arrow in Figure 8a indicates the gap where the dipole will form.

to the jet in the gap resulting in the formation of a weak dipole that disappeared after a short period. Fluid peeled off the outer edge of the remnant of the original vortex and formed a streamer that entered the gap positioned just south (named here for convenience $\text{gap}_{\text{South}}$) of the gap where the dipole formed. This fluid formed a new cyclonic vortex in the wake of the cylinder (Figure 6b), causing bifurcation of the original vortex into two vortices with the same mechanism described in section 1.2 and observed in the work of *Cenedese* [2002], *Adduce and Cenedese* [2004], and *Cenedese et al.* [2005]. Eventually, both the weak dipole and the original vortex disappeared and the interaction resulted in the production of a relatively large cyclonic vortex. In some experiments, the whole remnant vortex was able to pass through $\text{gap}_{\text{South}}$ and a streamer and a new vortex did not form. A dipole was never observed to form at the $\text{gap}_{\text{South}}$.

[19] The different behavior observed for different values of the parameter D_{isl}/d can be explained as follows. For large D_{isl}/d (i.e., $0.5 < D_{isl}/d \leq 1.5$), the original cyclonic vortex fluid is funneled through the gap for a long time interval before the remnant of the original vortex reaches the $\text{gap}_{\text{South}}$. Hence, the dipole generation is complete with a resulting strong cyclonic part of the dipole (Figure 6a). On the other hand, for small D_{isl}/d (i.e., $0.2 < D_{isl}/d \leq 0.5$), a short time after the original vortex fluid is funneled through the gap, forming a dipole, the remnant of the original vortex could be moving in front of $\text{gap}_{\text{South}}$ and start forming a new streamer (Figure 6b). Consequently, the formation of the dipole at the gap just north of $\text{gap}_{\text{South}}$ will be interrupted and not complete, resulting in a weak dipole that will soon disappear.

[20] The shape of new cyclonic vortex was often significantly distorted (e.g., Figure 7d). The formation of large vortices downstream of the cylinders is surprising as the gap width was only between 10 and 40% of the initial vortex diameter. For larger values of G/d, the new cyclonic vortex had sufficient energy to reach the western wall of the tank, while for the smaller values of G/d, the dipole (when formed) was small and weak (compared with that observed for larger values of G/d), and hence the new cyclonic vortex decayed far from the western wall of the tank. For large values of G/d the number of new cyclonic vortices, N, was 1 in most cases, rarely 2, and never 0, while for small values of G/d, N was 1 (seldom 0) and no backward flow was

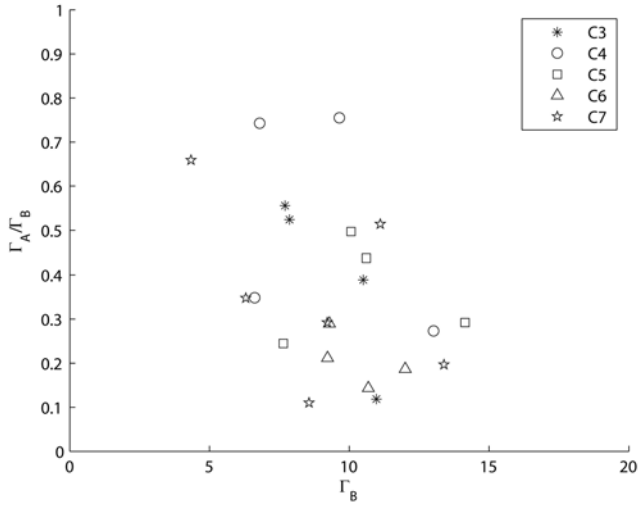

Figure 9. Γ_A/Γ_B versus Γ_B. Γ_B and Γ_A are the vortex circulations before and after the interaction, respectively. The different symbols represent the configurations of the cylinders illustrated in Figure 5.

observed. Finally, Figure 9 suggests that the relative reduction of vortex intensity (i.e., circulation) tends to be large (small Γ_A/Γ_B where the subscripts A and B indicate "after" and "before," respectively) for intense vortices (large Γ_B).

3.2. No Dipole Formation or Vortex Bifurcation ($0.03 \leq G/d \leq 0.1$)

[21] For values of $0.03 \leq G/d \leq 0.1$, when a vortex encountered the chain of cylinders, a small portion of the vortex fluid leaked through the gaps, but neither a dipole nor a new cyclonic vortex in the wake of the cylinders was observed to form (i.e., always $N = 0$), for all the configurations of the cylinders and Y_{dis}.

[22] The reason why the new vortex and dipole generations were suppressed for $0.03 \leq G/d \leq 0.1$ and were reduced for values of $G/d \sim 0.2$, might be explained by considering the thickness of the boundary layers over the vertical walls of the cylinders. (We are interested in only the zonal boundary layers since the flow through the gaps is zonal.) On the f-plane, the boundary layer thickness δ is expressed as

$$\delta = LE_H^{\frac{1}{2}}/E_L^{\frac{1}{4}} = \nu^{\frac{1}{4}}H^{\frac{1}{2}}/\Omega^{\frac{1}{4}}, \tag{7}$$

where $E_L = \nu/(\Omega L^2)$ is the Ekman number based on the horizontal length scale L, $E_H = \nu/(\Omega H^2)$ is the Ekman number based on the vertical length scale H, and Ω is the rotation rate of the system. In the laboratory, $\nu = 0.01$ cm^2 s^{-1}, $\Omega = f/2 = 0.125$ s^{-1}, $L = D = 3.3$ cm, and $H = h_0 \approx 10$ cm. Therefore $\delta = 1.68$ cm. On the β-plane, two kinds of zonal Ekman boundary layers exist, namely

$$\delta_{zonal,m} = \left(\delta_m^3 L\right)^{\frac{1}{4}}, \qquad \delta_{zonal,s} = \left(\delta_s L\right)^{\frac{1}{2}}, \tag{8}$$

where $\delta_m = (\nu/\beta_0)^{\frac{1}{3}}$ is the Munk boundary layer, $\delta_s = r/\beta_0$ is the Stommel boundary layer, $r = \delta_{Ek} f/(2H)$ is the linear friction coefficient, β_0 is the beta parameter, and $\delta_{Ek} = \sqrt{2\nu/f}$ is the bottom Ekman layer depth. $\beta_0 = sf/H = 0.0125$ s^{-1} cm^{-1} in the laboratory. Thus, we have $\delta_{zonal,m} = 1.26$ cm, $\delta_{zonal,s} = 0.97$ cm. Hence, the largest thickness of these zonal boundary layers is the f-plane b. One thickness $\delta = 1.68$ cm. For $G/d \lesssim 2\ \delta/d$ the viscous boundary layers occupy the entire region within each gap. We expect that the presence of the boundary layers will decrease the velocity of the fluid within the gaps, reducing the values of the Reynolds number of the jet in the gap (i.e., Re_G), and/or of the streamer going around the cylinder in a counterclockwise direction (i.e., Re). Hence, we anticipate that the criteria for dipole formation ($Re_G > 200$) [*Cenedese et al.*, 2005] and for the new vortex formation in the wake of the cylinder ($400 \leq Re \leq 1100$) [*Cenedese*, 2002] are no longer satisfied for $G/d \lesssim 2\ \delta$/d. For vortex sizes varying between 7.6 and 19 cm (section 2.1), the parameter $2\ \delta/d$ varied between 0.17 and 0.44; hence, we would not expect a dipole or a new vortex to form for $G/d \lesssim 0.1$, as confirmed in our experiments.

4. Comparison With Previous Laboratory and Numerical Studies

[23] The formation of dipoles observed for $0.1 < G/d \leq 0.4$, has not been observed in previous numerical simulations by *Simmons and Nof* [2002] and *Wang and Dewar* [2003] or in the analytical work of *Johnson and McDonald* [2004a, 2004b, 2005]. However, dipole formation was observed to occur, for similar values of G/d, in the work of *Cenedese et al.* [2005] and in laboratory experiments focusing on the generation of dipoles from a jet [*Afanasyev and Korabel*, 2004; *Afanasyev*, 2006]. The major difference between the laboratory experiments and the numerical simulations and analytical work referenced above, is the lack of viscosity in the numerical and analytical studies, i.e., only inviscid fluid were investigated. A jet produces vorticity when entering a quiescent fluid only if the fluid is viscous, consequently generating a velocity shear (i.e., vorticity) at the edges of the jet. In an inviscid fluid, vorticity cannot be generated by this mechanism. Hence, the above discrepancy is expected. In the MICOM (viscous) numerical simulations (E. Chassignet, personal communication, 2004) of the Caribbean region, dipoles are observed downstream of the Lesser Antilles and propagate westward into the Eastern Caribbean Sea (Sea Surface Height Anomaly movies, available at http://oceanmodeling.rsmas.miami.edu/micom). However, it is not clear if they are formed by the same mechanism as observed in the laboratory. The simulations have a 1/12° resolution (∼10 km) and the gaps are only 30–60 km wide; it could be possible that the simulations do not resolve the dynamics observed in the laboratory and higher-resolution runs may be necessary. On the other hand, more conclusive results could be obtained by examining the details of the model output.

[24] The bifurcation of the original vortex with the generation of a new vortex downstream of the islands, observed in the present experiments for $0.1 < G/d \leq 0.4$ and $0.2 < D_{isl}/d \leq 0.5$, was observed in some of the previous numerical and analytical work. The same behavior was also observed to occur in the laboratory by *Cenedese* [2002] for $0.2 \leq D/d \leq 1.0$, consistent with the values of D_{isl}/d mentioned above. The mechanism for vortex bifurcation discussed in section 2.1, invoking the circulation

around a closed contour, relies on viscosity (equation (1)). Hence, we believe that the bifurcation mechanism is different between the laboratory and the numerical and analytical inviscid studies, which would explain why the parameter ranges for vortex bifurcation are not the same. In particular, *Simmons and Nof* [2002] observed the original vortex to bifurcate into multiple vortices for values of $L/R_i = 1.5$, where L is the island length, R_i is the initial vortex radius. The equivalent parameter in the present study is the ratio $\Lambda = D_{isl}/r$. Contrary to their results, we could not find any relationships between Λ and N (the number of new vortices) which in most cases was $N = 1$. Nevertheless, we did observe that for small values of Λ, a backward flow existed, indicating that the vortex did not "notice" the existence of the islands, in agreement with the results of *Simmons and Nof* [2002] for small L/R_i and of *Cenedese* [2002] for $D/d < 0.2$. In agreement with *Simmons and Nof* [2002], we observed that intense vortices experience a relatively larger intensity loss than weaker vortices, as shown in Figure 9. In the MICOM simulations, new vortices are observed to form regularly downstream of the islands. From the model output movies of Sea Surface Height Anomaly, it is not possible to be conclusive as to the formation mechanism for the new vortices. The laboratory results suggest what may be observed in the MICOM simulations, but possibly higher resolution regional simulations may be necessary to resolve the dynamics observed in the laboratory.

[25] Finally, it is worth noticing that the present result obtained for values of $0.03 \leq G/d \leq 0.1$, indicating that a small portion of the vortex fluid leaked through the gaps but neither a dipole nor a new cyclonic was observed to form, has not been observed by *Simmons and Nof* [2002]. In their study, the vortex fluid always reorganized downstream of the island chain either as a single vortex or as multiple vortices.

5. Comparison With Observations

[26] In order to compare the laboratory results to oceanographic observations, the relevant nondimensional parameters must be evaluated. As discussed in section 2.1, the relevant nondimensional parameter is the Reynolds number of the streamer (Re), for a new cyclonic vortex to form in the wake of the cylinder, or the Reynolds number in the gap (Re_G), for a dipole to form downstream of the cylinders. Furthermore, in rotating viscous flows, the Rossby and Ekman numbers indicate the relative importance of advection on rotation, and viscous forces on rotation, respectively. As in previous similar laboratory experiments [*Cenedese*, 2002; *Adduce and Cenedese*, 2004; *Cenedese et al.*, 2005] the Rossby number of the cyclonic flow in the laboratory was approximately constant $Ro \sim 0.6–1$, values slightly larger than those observed for the NBC rings having $Ro \sim 0.2 – 0.4$. The vertical Ekman number $E_H = \nu/(\Omega H^2) = 8 \times 10^{-4}$ (section 3.2) in the laboratory while in the ocean $E_H = 10^{-8}$, using the kinematic viscosity of water, $f = 10^{-4}$ s^{-1}, and $H = 1000$ m or $E_H = 10^{-4}$, using a "turbulent" viscosity, $\nu_T = 0.01$ m^2 s^{-1}. While we can be conclusive in stating that the laboratory experiments have similar values of Rossby number as in the ocean, the value of the Ekman number in the ocean varies considerably. Regardless, both in the laboratory and in the ocean the Ekman number is small. This ambiguity in assigning a value of viscosity to the ocean is the reason why we choose to use "geometrical" nondimensional numbers (i.e., G/d and D_{isl}/d) in the discussion of the laboratory results rather than the values of the Reynolds numbers Re and Re_G. In the ocean, the Reynolds number, based on the kinematic viscosity, is very large (O (10^{10}), when using a velocity scale of 1 m s^{-1} and a gap width of 40 km) and clearly cannot be reproduced in the laboratory. However, it is well known that turbulent flows involve large scale structures, and it is fundamental that similar behaviors are observed in the laboratory. For example, one can observe Karman vortex streets in the wake of an island both in the ocean and in the laboratory; hence, the "effective" Reynolds number in the ocean must take into account the turbulent structures and an appropriate "turbulent" viscosity is necessary. If one were to use the value of $\nu_T = 0.01$ m^2 s^{-1}, the "gap" Reynolds number would decrease four orders of magnitude to $Re_G = 4 \times 10^6$. This value is still larger than that observed in the laboratory but is clearly dependent on the value attributed to ν_T. Given the somewhat arbitrary choice for the value of the "turbulent" viscosity, we will compare the laboratory results and the oceanic observations in terms of the geometrical nondimensional parameters, G/d and D_{isl}/d, which are straightforward to evaluate in oceanographic applications. The values of G/d and D_{isl}/d can be related to Re_G and Re, respectively. In section 1.2 we discuss the dependence of Re on D_{isl}/d (equation (5)). In section 3.2, we discuss how Re_G depends on the value of G/d. That is, for values $G/d \lesssim 2\,\delta/d$, the velocity in the gap, and hence Re_G, is decreased by the presence of boundary layers. On the other hand, for larger G/d ($\gtrsim 0.4$), the vortex fluid funneled into a larger gap will also have a lower velocity (i.e., lower Re_G) as shown in the work of *Cenedese et al.* [2005]. (In the present experiments it was not possible to measure directly the value of Re_G as in the work of *Cenedese et al.* [2005] because the velocity field encompassed the whole island chain (the velocity in the single gaps was not resolved). As discussed in section 2.2, a spatial average over 2 cm was used to obtain the gridded velocity, while the maximum width of each gap was only 3.3 cm.) In summary, we believe that the laboratory experiments are insightful in understanding the interaction of NBC rings with the Lesser Antilles and that they capture the essential dynamics of the interaction.

[27] The Lesser Antilles have passages' between 30 and 60 km wide and many of the islands have a spatial scale of approximately 80 km, with some larger obstructions (such as the Grenadines) that reach 225 km. The approaching NBC vortices' diameter varies between 200 and 400 km [see *Fratantoni and Richardson*, 2006]. The two geometrical nondimensional parameters discussed in section 3.1 for NBC rings interacting with the Lesser Antilles are $0.07 < G/d < 0.3$ and $0.2 < D_{isl}/d < 0.4$. The results discussed in section 3 suggest that both dipole formation and bifurcation of the original vortex, with the generation of a single vortex in the wake of an island, should occur when an NBC ring interacts with the islands of the Lesser Antilles. The value of the parameter $2\,\delta/d$ is approximately 10^{-3}, smaller than the values of G/d observed for the Antilles gaps; hence, the boundary layers in the oceanographic gaps should never prevent a dipole or a new vortex to form, as described in section 3.2. However, given the dependence of δ on ν_T, the boundary layer width, δ, could be

larger and possibly prevent the formation of dipoles and new vortices in the narrowest of the Lesser Antilles passages. The drifter studies of *Fratantoni and Richardson* [2006] and *Richardson* [2005] indicate that many surface drifters move through the passages of the Lesser Antilles into the East Caribbean Sea. In particular, the drifter trajectories [*Fratantoni and Richardson*, 2006] indicate that the NBC rings are destroyed east of the islands and only filaments of ring core fluid are able to enter the eastern Caribbean. These filaments could be the oceanic counterpart of the ''streamers'' and ''jets'' observed in the present laboratory experiments. However, from the drifter tracks it was not possible to discern the formation of dipoles or new vortices in the wake of the islands. Nevertheless, Figure 2, from *Richardson* [2005], is suggestive that both cyclones (blue) and anticyclones (red) are forming in the wake of the Lesser Antilles. In summary, the relevant geometrical nondimensional numbers, G/d and D_{isl}/d, suggest that a mechanism similar to that observed in the present experiments, producing dipoles and new vortices in the wake of the island chain, could be occurring when a NBC ring interacts with the Lesser Antilles. The available observations do not confirm nor dispute this suggestion.

6. Summary and Conclusions

[28] Laboratory experiments have been carried out to investigate the physical processes that govern the interaction of a self-propagating barotropic cyclonic vortex with aligned vertical circular cylinders. The motivation of the present work was the ''unexpected'' formation of a dipole in the work of *Cenedese et al.* [2005]. In particular, the study here focused on two features that rely on the presence of an island chain and could not have been investigated by *Cenedese et al.* [2005] with only two islands. First, we investigated the possibility of multiple dipole formation from a single vortex, and the potential interaction of these dipoles, as described in the working hypothesis (section 1.3) and in Figure 3. Second, we investigated the fate of a vortex interacting with an ''island chain'' for values of $G/d \rightarrow 0$, expecting the bifurcation and dipole formation mechanisms to stop occurring as $G/d \rightarrow 0$.

[29] The geometrical nondimensional parameters which regulated the flow in the experiments were the ratio of the gap size to the diameter of the incident vortex, G/d, and the ratio of the island diameter to the diameter of the vortex, D_{isl}/d. For $0.1 < G/d \leq 0.4$, after the vortex interacted with the cylinders, a dipole was observed to form downstream of one of the gaps in most experiments, for all the configurations of the cylinders and the initial vortex positions, Y_{dis}. After the dipole formed, the cyclonic part of it became dominant. For values of $0.1 < G/d \leq 0.4$ and $0.2 < D_{isl}/d \leq 0.5$, the interaction was either similar to the one described above, or, in some experiments, the dipole formation was interrupted and a streamer formed and entered the gap positioned just south of the gap where the dipole formed. Hence, a new cyclonic vortex formed in the wake of the cylinder (Figure 6b), causing the bifurcation of the original vortex into two vortices with the same mechanism as observed in the work of *Cenedese* [2002], *Adduce and Cenedese* [2004], and *Cenedese et al.* [2005]. The size of the dipole was larger for larger values of G/d, and each vortex in the dipole was smaller than the incident vortex. The number of new cyclonic vortices downstream of the cylinders, N, was one in general, independently of the parameter Λ, in disagreement with the results of *Simmons and Nof* [2002]. However, intense vortices were found to experience relatively greater amplitude loss than weak vortices, in agreement with the results of *Simmons and Nof* [2002]. An unexpected and new result of this study is that the formation of two or more dipoles never occurred. As described in section 3.1, the dipole forms only downstream of the gap aligned with the northernmost part of the vortex where the vortex azimuthal velocity is directed westward. We expected multiple dipoles to form when the original vortex interacted with multiple gaps. However, this was not the case, and even if the original vortex overlapped multiple passages, only a single dipole formed. Consequently, we did not observe any dipole interactions.

[30] For values of $0.03 \leq G/d \leq 0.1$, a different phenomenon was observed. When a vortex encountered the cylinders, a small portion of fluid in the vortex leaked through the gaps but neither a dipole nor a new cyclonic vortex formed downstream of the cylinders. This behavior is likely due to the presence of boundary layers over the vertical walls of the cylinders at the gaps as suggested by $G/d \lesssim 2\,\delta/d \sim 0.1$. The flow velocity in the gap could be reduced producing a lower value of the Reynolds number, and the suppression of both the dipole and vortex formation. This new result indicates that the interaction of a cyclonic vortex with aligned cylinders can result in the destruction of the original vortex by slowly leaking fluid through the passages, without reorganizing into a coherent vertical structure.

[31] The large anticyclonic and cyclonic vortices observed in the Eastern Caribbean Sea [*Richardson*, 2005] are thought to be generated by the interaction of NBC rings with the Lesser Antilles islands. Since the Lesser Antilles' passages have values of $0.07 \leq G/d \leq 0.3$, our experimental findings suggest that one dipole may be formed at one of the Lesser Antilles' passages when a NBC ring (anticyclone) collides with the islands. The dominant anticyclonic offspring may be formed either directly from the anticyclonic part of the dipole or from the remnant of the original vortex. The result of the present experiments indicating that no vortices were formed for $G/d \lesssim 2\,\delta/d \sim 0.1$ suggests that for small enough island passages, no vortices should form in the ocean due to the presence of boundary layers that can slow the fluid within the gaps. This hypothesis is hard to prove because the oceanic ''turbulent'' viscosity ν_T is not known exactly. An estimate for the ocean is $2\,\delta/d \sim 10^{-3}$, smaller than the values of G/d but, given the uncertainties on the value of δ, suppression of dipole and vortex formation could occur in some passages as may be suggested by drifter trajectories [*Fratantoni and Richardson*, 2006].

[32] In the present study, the vortices used were cyclonic and barotropic. Moreover, they approached perpendicularly the chain of circular cylinders. On the contrary, in the ocean, NBC rings are anticyclonic and baroclinic vortices moving along an oblique direction to the island chain. Furthermore, the islands' shape might be different from being cylindrical, and the local bottom topography is much more complicated. These, together with a lower Reynolds number than that observed in the ocean, are some of the limitations of the present experiments and it would be interesting to see how the results reported in this paper could be modified by the

inclusions of these details (i.e., anticyclonic vortices, baroclinicity, direction of propagation, various shapes of each of the islands, inclusion of barriers (i.e., sills) at the gaps of the islands) in the laboratory experiments. However, the experiments here do capture the fundamental dynamics of the interaction of a vortex with an island chain and bring new and original insight to better understand this complex process.

[33] To date there is a lack of information on the fate of the water within the NBC rings "leaking" into the eastern Caribbean via the Lesser Antilles islands' passages. Direct observations of the flow through the Lesser Antilles passages are needed to clarify if dipoles or new vortices are generated downstream of the passages after an NBC ring interacts with the island chain. Recent numerical models (E. Chassignet, personal communication, 2004) investigating the interaction of NBC rings with the Lesser Antilles did not focus on this particular scenario and a collaborative study linking laboratory, numerical, and observational studies may be necessary to bring new insight on the relevant dynamics regulating the fate of the water mass in the NBC rings.

[34] **Acknowledgments.** We acknowledge the hospitality of the 2005 Program in Geophysical Fluid Dynamics (GFD) at Woods Hole Oceanographic Institution where this work was completed. A.T. was supported by GFD Summer Fellowship 2005. The laboratory experiments were carried out with the capable assistance of Keith Bradley.

References

Adduce, C., and C. Cenedese (2004), An experimental study of a monopolar vortex colliding with topography of varying geometry in a rotating fluid, *J. Mar. Res.*, *62*, 611–638.

Afanasyev, Y. D. (2006), Formation of vortex dipoles, *Phys. Fluids*, *18*, 037103.

Afanasyev, Y. D., and V. N. Korabel (2004), Starting vortex dipoles in a viscous fluid: Asymptotic theory, numerical simulations and laboratory experiments, *Phys. Fluids*, *16*, 3850, doi:10.1063/1.1790493.

Batchelor, G. K. (1967), *An Introduction to Fluid Dynamics*, p. 93, Cambridge Univ. Press, New York.

Cenedese, C. (2002), Laboratory experiments on mesoscale vortices colliding with a seamount, *J. Geophys. Res.*, *107*(C6), 3053, doi:10.1029/2000JC000599.

Cenedese, C., C. Adduce, and D. M. Fratantoni (2005), Laboratory experiments on mesoscale vortices interacting with two islands, *J. Geophys. Res.*, *110*, C09023, doi:10.1029/2004JC002734.

Cushman-Roisin, B. (1994), *Introduction to Geophysical Fluid Dynamics*, Prentice Hall, Englewood Cliffs, N. J.

Dewar, W. K. (2002), Baroclinic eddy interaction with isolated topography, *J. Phys. Oceanogr.*, *32*, 2789–2805.

Fratantoni, D. M., and D. A. Glickson (2002), North Brazil Current rings generation and evolution observed with SeaWiFS, *J. Phys. Oceanogr.*, *32*, 1058–1074.

Fratantoni, D. M., and P. L. Richardson (2006), The evolution and demise of North Brazil Current rings, *J. Phys. Oceanogr.*, *36*, 1241–1264.

Godfrey, J. S. (1989), A Sverdrup model of the depth-integrated flow from the world ocean allowing for island circulations, *Geophys. Astrophys. Fluid Dyn.*, *45*, 89–112.

Herbette, S., Y. Morel, and M. Arhan (2003), Erosion of a surface vortex by a seamount, *J. Phys. Oceanogr.*, *33*, 1664–1679.

Johnson, E. R., and N. R. McDonald (2004a), The motion of a vortex near a gap in a wall, *Phys. Fluids*, *16*, 462–469.

Johnson, E. R., and N. R. McDonald (2004b), The motion of a vortex near two circular cylinders, *Proc. R. Soc. London, Ser. A*, *460*, 939–954.

Johnson, E. R., and N. R. McDonald (2005), Vortices near barriers with multiple gaps, *J. Fluid Mech.*, *531*, 335–358.

Jones, W. E., T. N. Lee, F. A. Schott, R. J. Zantopp, and R. H. Evans (1990), The North Brazil Current retroflection: Seasonal structure and eddy variability, *J. Geophys. Res.*, *95*, 22,103–22,120.

Kloosterzil, R. C., and G. J. F. van Heijst (1991), An experimental study of unstable barotropic vortices in a rotating fluid, *J. Fluid Mech.*, *223*, 1–24.

Linden, P. F., B. M. Boubnov, and S. B. Dalziel (1995), Source-sink turbulence in a rotating stratified fluid, *J. Fluid Mech.*, *298*, 81–112.

McWilliams, J. C. (1984), The emergence of isolated coherent vortices in turbulent flow, *J. Fluid Mech.*, *146*, 21–43.

Pedlosky, J., L. J. Pratt, M. A. Spall, and K. R. Helfrich (1997), Circulation around island and ridges, *J. Mar. Res.*, *55*, 1199–1251.

Richardson, P. L. (2005), Caribbean current and eddies as observed by surface drifters, *Deep Sea Res. II.*, *52*, 429–463.

Simmons, H. L., and D. Nof (2000), Islands as eddy splitters, *J. Mar. Res.*, *58*, 919–956.

Simmons, H. L., and D. Nof (2002), The squeezing of eddies through gaps, *J. Phys. Oceanogr.*, *32*, 314–335.

Voropayev, S. I., and Y. D. Afanasyev (1994), *Vortex Structures in a Stratified Fluid*, Chapman and Hall, London.

Wang, G., and W. K. Dewar (2003), Meddy-seamount interactions: Implications for the Mediterranean Salt Tongue, *J. Phys. Oceanogr.*, *33*, 2446–2461.

Whitehead, J. A., M. E. Stern, G. R. Flierl, and B. A. Klinger (1990), Experimental observations of baroclinic eddies on a sloping bottom, *J. Geophys. Res.*, *95*, 9585–9610.

C. Cenedese, Department of Physical Oceanography, Woods Hole Oceanographic Institution, Woods Hole, MA 02543, USA. (ccenedese@whoi.edu)

A. Tanabe, Department of Mathematics, Imperial College London, London SW7 2AZ, UK.